Journal of Intelligent Systems with Applications 2025; 8(1): 5-13

Sensor Design and Low Cost APAP Design to Determine the Digital Rate of Nasal Air Duct Obstruction

Gurkan Bilgin[1,*]
[1]Department of Electrical and Electronics Engineering, Burdur Mehmet Akif University, Burdur, Turkey
ORCIDs: 0000-0002-8441-1557
E-mails: gbilgin@mehmetakif.edu.tr
*Corresponding author.

***Abstract*—Nasal air duct obstruction (NADO) is not only a mechanical narrowing or obstruction of the upper respiratory tract, but also a clinically important health problem with systemic effects. Obstruction of airflow through the nasal air canal causes impairment of some physiological functions and compels individuals to breathe through the oral. This may cause various disorders such as various upper respiratory tract infections, cardiovascular disorders, decreased sleep quality. Early diagnosis of NADO, confirmation with objective measurement methods and application of appropriate treatment approaches such as automatic positive airway pressure (APAP) device are critical for both providing symptomatic relief and maintaining overall health and quality of life. In this study, a system has been designed that can digitally determine the NADO condition that occurs due to chronic or acute reasons and after this determination, the air pressure of the APAP device can be adaptively adjusted according to this obstruction rate. The sensor designed in this study is intended to provide information about the ratio of breath that cannot pass through the nasal air canal and to provide sleep clinicians and physicians with helpful information about the condition of the disorder. This sensor is intended to send information to an APAP design to provide optimum air pressure as a result of evaluations.**

Keywords*—*nasal air duct obstruction; sensor design; infrared sensor; Arduino Mega

I. Introduction

The utilisation of electronic devices within the medical field has facilitated the precise diagnosis and treatment of numerous diseases and conditions, thereby ensuring their reliability. A significant number of developments in this field have resulted in the digitalisation and automation of medical research and clinical decision-making processes. In traditional societies, the approach to health, which was intertwined with culture, was based more on experiential knowledge than on a scientific perspective. In the modern era, the primacy previously held by experiential and dogmatic knowledge has been superseded by that of scientific knowledge, with the field of health being comprehensively absorbed into the domain of science [1].

In addition to its functions such as warming, humidifying, and filtering the air during respiration, and detecting odours, which is one of its most significant tasks, the nose is also crucial for pulmonary functions [2]. Nasal obstruction, otherwise known as upper respiratory tract narrowing, may be caused by a number of factors including anatomical abnormalities, inflammation, infection, or allergies. This condition, if left untreated, can result in impaired respiratory function. Nasal air duct obstruction (NADO) has been demonstrated to have a significant impact on sleep quality, leading to the occurrence of snoring. Furthermore, it has been associated with an increased risk of developing Obstructive Sleep Apnoea (OSA) and cardiovascular disorders [3], [4]. Research into the causes of respiratory problems in humans, and efforts to find solutions, have been a significant area of study from the past to the present day. Inadequate breathing has been demonstrated to be a causal factor for numerous health complications, including but not limited to myocardial infarction, tachycardia and dyspnoea [5]. The diagnosis of NADO is initiated through a detailed review of the patient's medical history and a comprehensive physical examination. Flexible or rigid endoscopy is frequently utilised to visualise the nasal cavity and nasopharynx. Furthermore, computed tomography (CT) and magnetic resonance imaging (MRI) techniques are utilised by physicians to facilitate surgical planning and enhance comprehension of soft tissue [6]. The treatment approach is meticulously designed according to the underlying causative factors. The utilisation of topical nasal corticosteroids, oral and topical antihistamines, and decongestants is a common practice in medical treatment [7]. In cases where medical treatment proves ineffective, interventions such as septoplasty, endoscopic sinus surgery and turbinate reduction surgery may offer a more effective solution [8], [9]. In certain cases, medical professionals may propose remedial measures that offer immediate relief during sleep and long-term treatment. Positive airway pressure (PAP) treatment, which provides a specific positive end-expiratory pressure (PEEP) to keep the airways open, is quite common in the treatment of sleep apnoea [10], [11]. For example, the Continuous Positive Airway Pressure (CPAP) device maintains air passageways open by providing constant pressure in the treatment of OSA and is now a standard approach [12], [13]. The air supplied to CPAP devices is typically within a pressure range of 4–20 cmH_2O. The pressure of the air is measured by sensors prior to its application to the patient, with the objective of determining the most appropriate pressure for the given circumstances [14]. Automatic Positive Airway Pressure (APAP) is a system that automatically adjusts its pressure according to the resistance exhibited by the airway due to causes such as apnoea, hypopnoea, and snoring during breathing, and provides the most suitable air pressure to the patient [15]. It has been demonstrated that CPAP and APAP are effective in reducing the apnoea-hypopnoea index (AHI) when utilised over an extended period in the treatment of OSA [16]. The distinction between a Bilevel Positive Airway Pressure (BPAP) device and a CPAP device lies in the former's ability to generate distinct pressures during inhalation and exhalation throughout the breathing cycle, subsequently supplying these pressures to the patient. The objective of this procedure is to enhance the patient's tolerance to positive pressure and facilitate their adaptation to the device [14]. APAP devices are described as devices with variable pressure. These devices have been shown to detect conditions that result in respiratory distress, including but not limited to, airflow restriction, sleep apnoea, and snoring, and to adjust the pressure accordingly [14]. It has been observed that APAP is more efficacious in circumstances requiring variable pressure, such as sleep position, weight fluctuations, and allergic reactions [17]. Moreover, it has been observed that the APAP device may enhance adherence to certain treatments, while in some studies, it may not demonstrate a significant impact on patient compliance [18].

From an engineering design perspective, APAP and CPAP devices incorporate components such as airflow sensors, data processing algorithms, and pressure regulators. Abbasnejad et al. demonstrated the applicability of the MEMS-based LCP flow sensor in the treatment of sleep apnoea. The findings show that the sensor can reliably monitor respiration with a lower detection threshold and higher sensitivity than commercial equivalents [19]. In a separate study, the alterations in nasal cavity volumes subsequent to isotonic physical exertion were analysed by means of acoustic rhinometry [20]. Kryger et al. developed a system for the collection and recording of data on diaphragm movements during breathing. This system was designed for use in studies of sleep apnoea and chronic obstructive pulmonary disease (COPD). In the study, diaphragm movements were meticulously recorded and evaluated using an accelerometer [21]. A study on the ergonomic design of CPAP revealed that it is feasible to develop customised CPAP masks using low-cost 3D scanning and production methods. The findings indicate that customised masks have significant potential to increase patient comfort and treatment compliance in CPAP therapy [22].

The significant expense of PAP devices available on the market creates a financial obstacle for patients with low income [23], [24]. In this study, a sensor design was developed to digitally demonstrate the restriction of airflow during breathing in patients with NADO. NADO can be caused by narrowing or obstruction in the upper respiratory tract due to anatomical, inflammatory, infectious, allergic, or other causes. The development of a low-cost, adaptive APAP device has been made possible by a sensor design that digitally determines the level of obstruction. This innovation enables the device to deliver air at the optimum pressure for the patient, based on the level of obstruction.

II. Materials & Methods

The system designed in this study is principally structured around three main functional units. The measurement, evaluation and pressure adjustment units are presented in the following section. The sensor, which has been designed to be incorporated into the measurement unit, aims to digitally determine the obstruction of the nasal air duct in individuals diagnosed with NADO. The sensor design is based on a distance sensor that operates using infrared technology. The sensor is located at the base of a specially designed cylindrical tube, which permits airflow and contains a ball that can move up and down with each breath. The device has been selected for the purpose of detecting the ball's height with each respiratory cycle. The evaluation of sensor data will be facilitated by the Arduino MEGA 2560. According to the evaluation results, the motor that provides the pressurized air to be supplied to the patient and the heated humidification system that provides humid air are being controlled. In the designed system, apparatus such as a nasal mask, tube, and filter have also been selected to ensure that the air reaches the patient in a healthy manner. The primary block diagram of the study is presented in Fig. 1.

Figure 1: Block diagram of the study

A. Sensing System with an Infrared Sensor

In this study, a sensor based on the volumetric calculation method was designed to determine the amount of air drawn in the detection of nasal duct obstruction of the patient. The design of the device was prepared from cylindrical mica, with a length of 80 cm and a radius of 2.3 cm. The device was closed with a grill, allowing air to pass through the base, and was mounted to the nasal mask with a flexible tubing system at the other end. The pipe has been coated with a matt material. A ball with a radius of 2.2 cm, weighing approximately 2 g, was placed in the mica tube to move freely. The infrared TOF200C-VL53L0X sensor, which is mounted on the base, can detect the distance based on the rise of the ball with each inhale.

As illustrated in Fig. 2, the mica pipe was utilised in the sensor system under consideration. As illustrated in Fig. 3, the grating system and infrared sensor have been positioned on the base of the pipe.

B. The Control Unit (Arduino Mega 2560)

The Arduino MEGA 2560, a microcontroller with open-source software, possesses 54 digital, 16 analogue pins and

Figure 2: Picture of the mica tube used in the designed sensor system

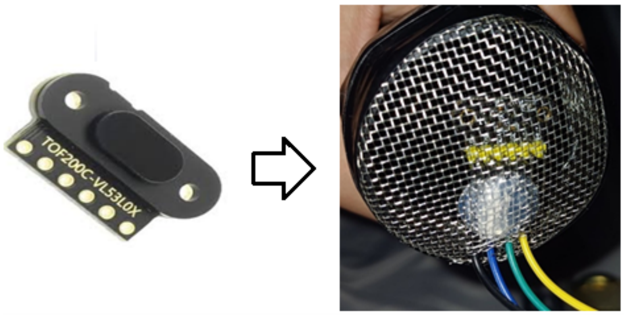

Figure 3: Infrared sensor and the grid placed at the base of the pipe

4 serial communication pins, rendering it optimal for studies incorporating a greater number of input and output elements [25]. Arduino's ease of use and the fact that it does not require special hardware for programming make it stand out among other platforms [26]. Thanks to their built-in voltage regulators, they are preferred in operations with a DC supply range of 6 to 20 volts [27]. Arduino boards have been commonly used in prototyping electronic circuits of many recent literature [28]–[36]. In this study, the Arduino MEGA 2560 microcontroller board was utilised to evaluate the data from the sensor and to control the air pressure motor in the event of insufficient air passage through the nasal duct. The Arduino MEGA 2560 is a microcontroller that can be used to facilitate the development of electronic systems.

C. Air Pressure Regulation Unit (Airflow Motor)

In the Adaptive APAP device, a brushless DC (BLDC) centrifugal blower motor was utilised to generate pressurised air for the APAP devices (Fig. 4). This motor, which is capable of operating both silently and at high speed, has an air flow rate of 100-200 L/min, and can operate within a pressure range of 3-30 cmH_2O and a speed range of 20,000-70,000 rpm. The sound level, ranging from 25 to 30 dB, has been found to be comfortable for patients during sleep. The BLDC driver card was utilised to facilitate the operation of the motor. The motor's electronic commutation is facilitated through a three-phase MOSFET bridge circuit and driver integration, while speed control is achieved through the PWM signal received from the microcontroller. Consequently, the integration of a BLDC blower motor, a BLDC driver board, and an Arduino Mega 2560 microcontroller within this structure facilitates the automatic adjustment of pressure in accordance with the patient's respiratory patterns.

Figure 4: Airflow motor used in the design

D. Humidification System

The humidifier with heater was used to humidify the air to be sent to the user. The 2.8" TFT Shield LCD display is an energy-efficient display type that functions with natural light-emitting diode (LED) technology. In the context of Arduino projects, the 2.8" TFT Shield LCD display is utilised for the purposes of visualising sensors and the creation of user layers. In this study, it was used to digitally display the air pressure delivered by the APAP device, the breath that the user can take through the oral and nasal, and the percentage of nasal obstruction.

E. Nasal Mask and Connection Hose

The nasal mask and hose to be used in the design are shown in Fig. 5. It is usually designed for use in respiratory devices such as CPAP or APAP and is made of siliconised material. This mask, which covers the nose and mouth, can deliver oxygen concentrations of up to 50-60%. Silicone raw material makes the mask more resistant to air leaks at high pressures. In the present study, two nasal masks were utilised. The primary mask is utilised to ascertain the volume of air that is passing through the mouth and nose, respectively, while the secondary mask is donned subsequent to the removal of the primary mask, thereby enabling the patient to be administered pressurised air during sleep. The masks are connected to the device, which is designed to provide air flow. This device is connected to a hose made of flexible PVC material with an inner diameter of 19 mm.

Figure 5: Nasal mask and connection hose

F. Calculation Procedure and Flowchart

In order to digitally determine the nasal obstruction and adjust the pressurised air at the outlet of the designed device, it was first necessary to determine the location of the obstruction in the nasal air ducts. For this purpose, the ball was placed inside the mica tube will move up and down with each breath. The height at which the ball reaches its maximum during the user's routine inhalation and exhalation was determined by means of an infrared sensor in the base. The volume of air drawn in through the oral or nasal ducts was calculated by applying Equation (1) below, which is used to find the volume of cylindrical bodies, to the height 'h' between the start of the ball and the point of maximum rise.

$$V_{air_n} = \pi \times r^2 \times h_n \tag{1}$$

According to Equation (1), "V_{air_n}" is the volume of air drawn in through the oral or nasal ducts, and "h_n" is the height "h" between the start of the ball and the point of maximum rise in the "n_{th}" breath. In order to calculate the obstruction of the nasal ducts, the amount of air inhaled from the mouth was taken as a reference value for the nose, with the logic that a healthy nose reaches the lungs as much as the breath inhaled through the mouth in each routine breathing. Consequently, the user is firstly requested to don the mask and breathe 10 times in a typical manner through the mouth to attain a standard through the mouth. In this process, the amount of incoming air in each breathing is calculated, and the mean value of the air volume is subsequently determined by the formulation in Equation (2). This value approximates the volume of air that the user should normally breathe through the unobstructed nose. The term 'V_M' is employed to denote the average of the air volumes breathed in through the mouth (a reference value for the nose).

$$V_M = \frac{1}{10} \times \sum_{n=1}^{10} V_{air_{n(mouth)}} \tag{2}$$

Subsequent to the process, the user is required to rest for a period of 10 seconds. Thereafter, the user is invited to close their mouth and breathe in and out 10 times via the nasal air ducts. Utilising a similar calculation method, the amount of air volume that the user can draw through the nose is calculated with the formulation in Equation (3). The term 'V_N' is used to denote the mean of the air volumes obtained from the nasal air channels.

$$V_N = \frac{1}{10} \times \sum_{n=1}^{10} V_{air_{n(nose)}} \tag{3}$$

Following these calculations, the digital percentage value of nasal obstruction is determined by calculating the ratio of 'V_M' and 'V_N' values to each other, as illustrated in Equation (4).

$$Nasal\ Obstruction = \frac{V_M - V_N}{V_M} \times 100\% \tag{4}$$

The positive air pressure to be applied is then adjusted by controlling the operation of the air pressure motor according to the nasal obstruction rate obtained. In consideration of the values cited in the extant literature [14], it was determined that the obstruction rate could be mapped onto the pressure range of 2-20 cmH_2O through linear scaling. A flow diagram showing the software explanation of the designed device is given in Fig. 6.

III. Experiments and Results

A considerable number of studies are currently being conducted in the field of biomedical device design. The devices and systems designed in this field make a significant contribution to the comfort and quality of life of human life with the benefits they provide on human health and disease diagnosis. In this study, an APAP device was designed to detect the percentage of nasal duct obstruction and adjust the air pressure given to the user accordingly. This device has been developed especially for patients with NADO and OSA problems in their daily lives. The values calculated with this device are displayed in Turkish language. An image of the completed designed device is given in Fig. 7.

Prior to the execution of measurement tests, the system presents a series of sequential messages to the user, thereby ensuring a comprehensible and methodical process. The values calculated and guidance with this device are displayed in Turkish language. Before commencing the measurements on the

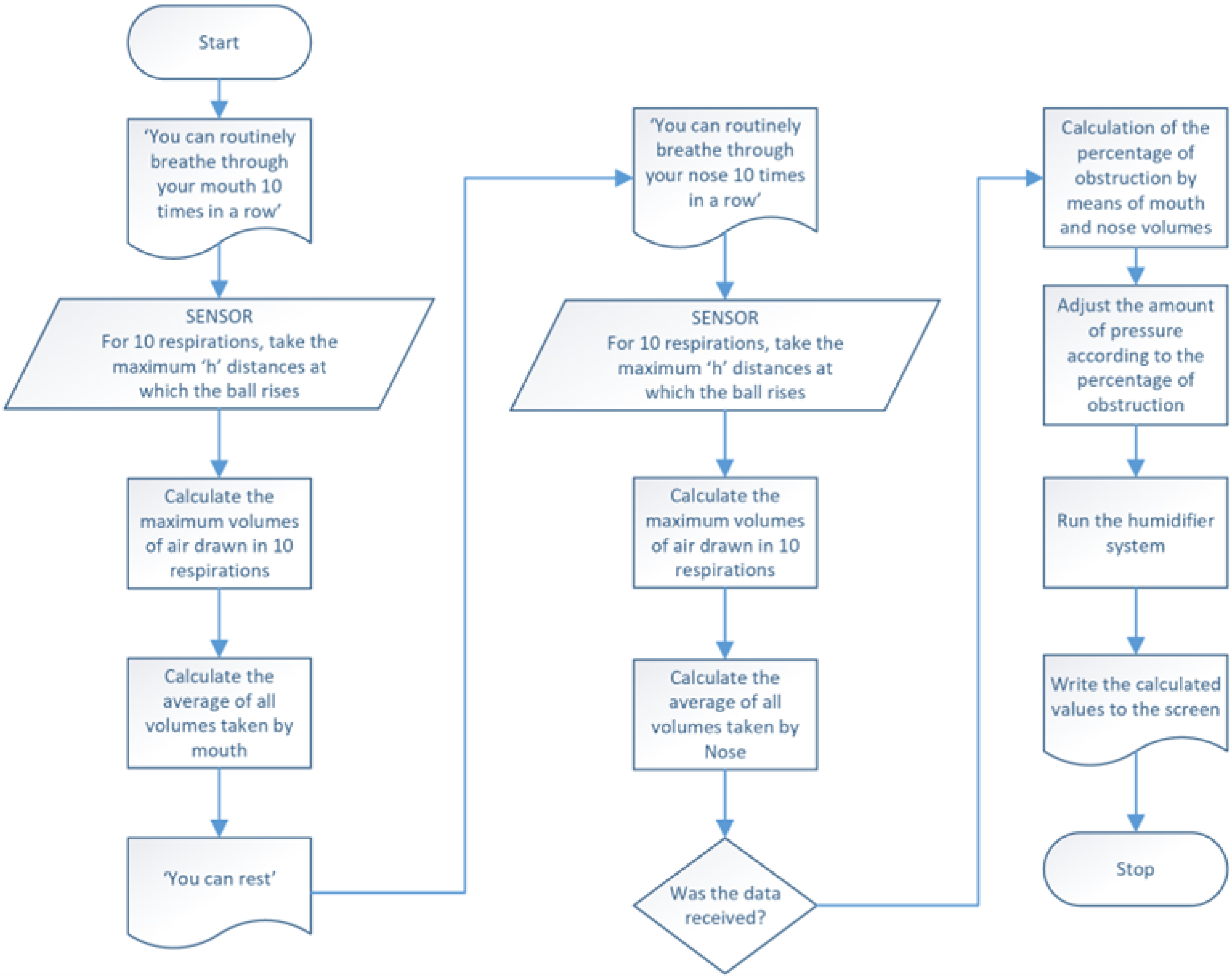

Figure 6: Flowcdhart of the designed system

LCD screen integrated into the design, the system displays the phrase 'You can breathe through the mouth'. Upon completion of the process, the LCD display will present the message 'You can rest', again followed by 'You can breathe through the nose'. Its display on the LCD screen is given in Fig. 8.

For the purpose of control, the tests were conducted with a user who did not have respiratory issues or NADO. Experiments were carried out on healthy nose with different rates of nasal air duct blockage scenarios. During the experimental procedure, the participant was firstly requested to undertake ten standard respiratory cycles, both in and out, via mouth. Thereafter, they were instructed to follow the phrase displayed on the screen, prior to conducting a further ten respiratory cycles, this time via the nasal cavity, following a period of rest.

In the absence of closing the nasal air duct, the mean rise of the ball within the sensor design was measured as 27.9 cm when breathing through the mouth and 27.3 cm when breathing through the nose. The air volume taken by the user through the mouth was calculated as 368.1 cm^3 and the air volume taken through the nasal air duct was calculated as 360.0 cm^3. The discrepancy between these two values was interpreted by the system as 2.2% as obstruction rate, and the theoretical support pressure corresponding to this rate was determined as 0.4 cmH_2O. The screenshot of the device displaying the results of this test is presented in Fig. 9.

The left nostril was occluded to a certain extent by external intervention with an apparatus, and the test was carried out with the scenario created. The measurement results of this scenario indicate that the average rise of the ball in the sensor design was 35.4 cm when breathing through the mouth and 24.8 cm when breathing through the nose. The air volume

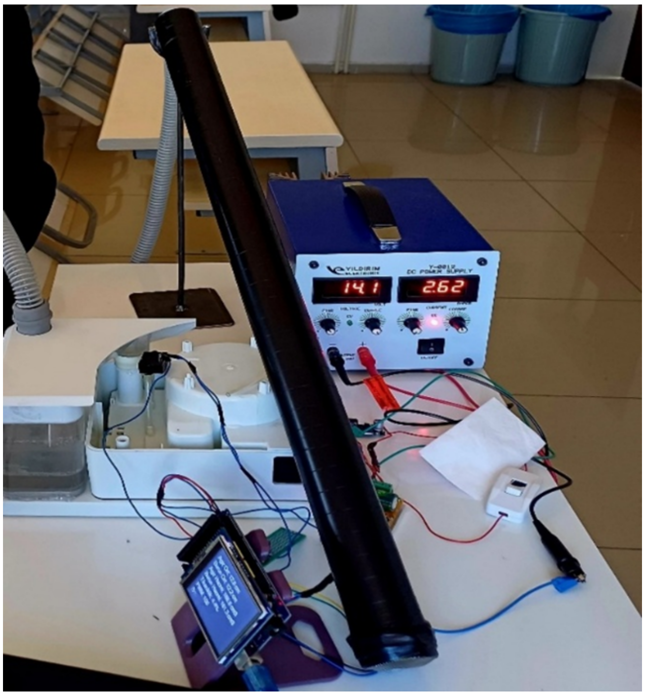

Figure 7: Photo of the designed APAP device

Figure 8: User guidance messages with LCD display

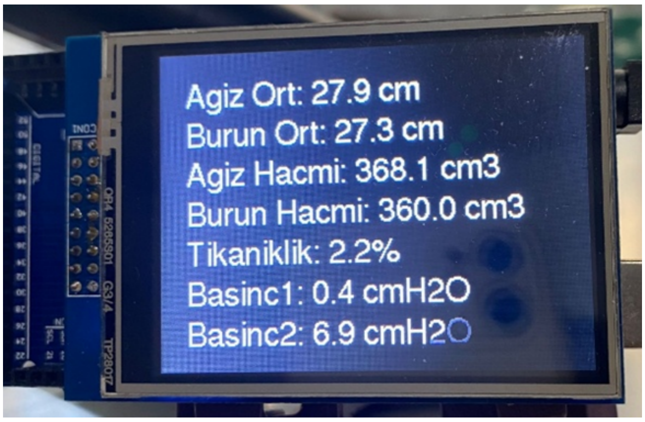

Figure 9: Test results with the nasal air ducts fully open

taken by the user through the mouth was calculated as 467.2 cm^3 and the air volume taken through the nasal air duct was calculated as 326.7 cm^3. The discrepancy between these two values was interpreted by the system as 30.1% as the obstruction rate, and the ideal support pressure corresponding to this rate was displayed on the screen as 6.0 cmH_2O. Left nostril restricted measurement results are given in Fig. 10.

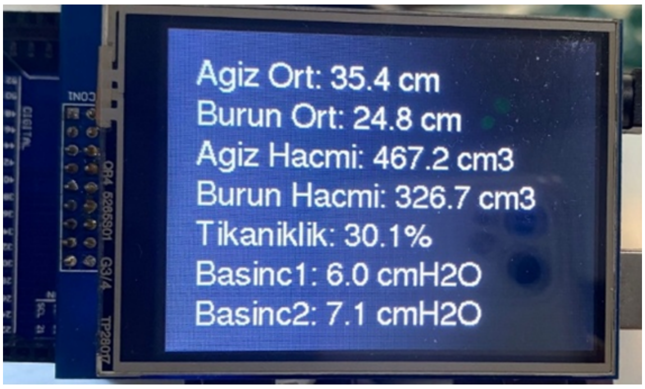

Figure 10: Test results with restricted left nostril

The right nostril was occluded to a certain extent by external intervention with an apparatus, and the test was carried out with the scenario created. The measurement results of this scenario indicate that the average rise of the ball in the sensor design was 29.3 cm when breathing through the mouth and 20.7 cm when breathing through the nose. The air volume taken by the user through the mouth was calculated as 386.5 cm^3 and the air volume taken through the nasal air duct was calculated as 273.8 cm^3. The discrepancy between these two values was interpreted by the system as 29.2% as the obstruction rate, and the ideal support pressure corresponding to this rate was displayed on the screen as 5.8 cmH_2O. Right nostril restricted measurement results are given in Fig. 11.

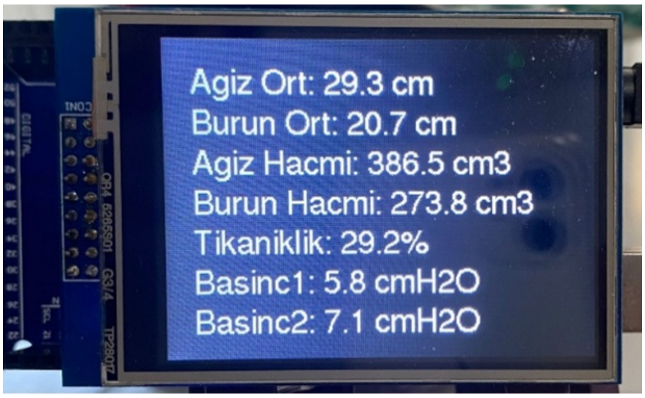

Figure 11: Test results with restricted right nostril

Both nostrils were occluded to a certain extent by external intervention with an apparatus, and the test was carried out with the scenario created. The measurement results of this scenario indicate that the average rise of the ball in the sensor design was 33.8 cm when breathing through the mouth and 7.4 cm when breathing through the nose. The air volume taken by the user through the mouth was calculated as 445.5 cm^3 and the air volume taken through the nasal air duct was calculated as 97.6 cm^3. The discrepancy between these two values was interpreted by the system as 78.1% as the obstruction rate, and the ideal support pressure corresponding to this rate was displayed on the screen as 15.6 cmH_2O. Both nostril restricted measurement results are given in Fig. 12.

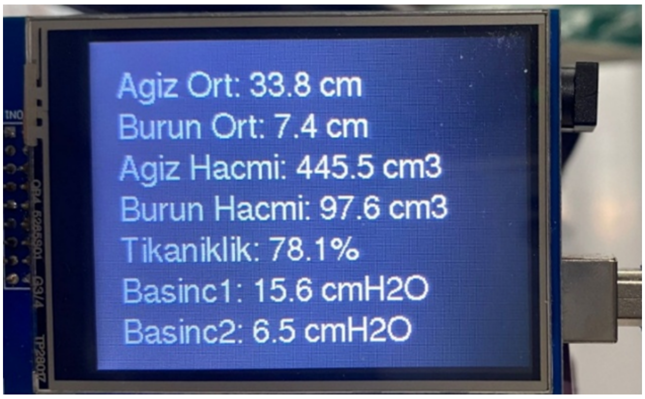

Figure 12: Test results with restricted both nostril

The results of the tests conducted with the nasal air ducts fully open, with the left nostril restricted, with the right nostril restricted, and with both nostrils restricted are presented in a comparative graph in Fig. 13.

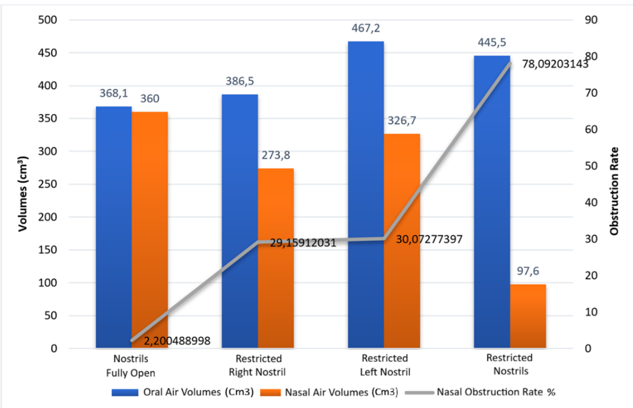

Figure 13: Comparative results for all scenarios

As demonstrated in Fig. 13, when both nostrils were unrestricted, the air volumes from the mouth and nasal air ducts exhibited extremely close values, thereby substantiating the finding of negligible obstruction with an obstruction rate of 2.2%. When evaluated separately in the right and left nostril restricted scenarios, there were noticeable decreases in the air volume taken from the nasal ducts, with these decreases resulting in congestion rates of 29.2% and 30.1%, respectively. These results show that the designed system is effective in revealing which of the two nasal ducts has problem-induced obstructions. In the scenario where both nostrils were restricted, the air volume extracted from the nasal ducts diminished to the lowest anticipated levels, amounting to 97.6 cm^3. The obstruction rate was consequently ascertained to be 78.1%. This demonstrates the system's capacity to respond accurately in different restricted scenarios and successfully detect severe blockages. The graph illustrating the air pressure values provided to the user in relation to the specified obstruction values is depicted in Fig. 14.

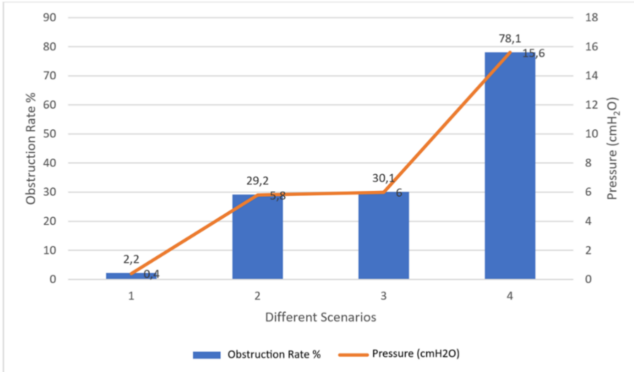

Figure 14: Pressure graph given to the user according to the percentage of nasal obstruction

As demonstrated by the graph, as the rate of nasal obstruction rises, the requisite positive air pressure concomitantly rises in proportion. While a low pressure of only 0.4 cmH_2O was recommended for an obstruction rate of 2.2%, this value increased to 15.6 cmH_2O for an advanced obstruction rate of 78.1%. This linear increase indicates that the pressure calculation algorithm employed in the system is both sensitive and adaptive. The system has been shown to maintain pressures within the range of 5.8-6.0 cmH_2O, which is considered to be within clinically acceptable parameters, particularly in cases of medium obstruction levels of around 29-30%. This outcome suggests that the system is able to avoid excessive intervention. However, in instances of high obstruction, the system has been observed to respond promptly, providing the necessary support.

IV. Conclusion

In this study, a system has been developed that has the capacity to digitally reveal the obstruction value of the nasal air ducts as a result of NADO occurring in the upper respiratory tract. Furthermore, the system has the capability to automatically generate positive air pressure according to this ratio. It is evident that the transmission of user instructions and measurement results to the user via the screen interface was effective in enhancing user-device compatibility and ensuring the reliability of measurement accuracy.

Upon analysis of the results, it was observed that the mean ball heights measured in the test measurements conducted without any nostril restriction and the calculated breath volumes accordingly yielded results that were closely aligned. This finding could be indicative of the absence of any restriction in the respiratory tract. The system calculations are predicated on the hypothesis that mouth and nose breathing are proximate phenomena. The results of the calculations demonstrate the veracity of this hypothesis. The model demonstrated its efficacy by successfully producing the anticipated outcomes in the low-level nostril obstruction scenario that was conducted for the purposes of evaluation. It yielded a comprehensible and lucid output for the user. The system was able to successfully detect restricted air passages through the nostril channel in separate nostril restriction scenarios. It was demonstrated that, consequently, the anticipated assistance was provided in the form of compressed air, at varying levels in accordance with the established obstruction rates. With these measurements, the system has demonstrated its sensitivity to the restriction of different nostrils. In scenarios where a high level of nostril restriction was performed in the final test, a significant level of pressurised air was produced, thus revealing this situation. When the graphs are interpreted, the fact that the measurement results provide consistent, meaningful and physiologically interpretable values reveals the potential for the system to be used diagnostically and therapeutically. Moreover, the observation that the algorithm demonstrates the correct bias even in circumstances of substantial occlusion serves to substantiate the assertion that the device under consideration is a reliable one, with the potential for enhancement through further detailed evaluation of patient data in future studies.

Today, the prices of these devices that provide commercial respiratory support in the field of health are quite high. Accessibility is therefore difficult. By means of the low-cost components used in this designed system, a device that is more economical and functional than the market and has potential in the field of health has been developed. With adequate enhancements and further patient research, there is potential for utilisation by low-budget users.

REFERENCES

[1] Turan Y. Uyku apnesi, hipertansiyon ve kardiyovasküler hastalıklar. Bozok Tıp Dergisi 2018; 8: 1-8.

[2] Eccles R. Nasal airflow in health and disease. Acta Oto-laryngologica 2000; 120(5): 580-595.

[3] Young T, Skatrud, J, Peppard, PE. Risk factors for obstructive sleep apnea in adults. JAMA 2004; 291(16): 2013-2016.

[4] Gokce G, Veli I, Yuce YK, Isler Y. Efficiency evaluation of rapid maxillary expansion treatment on nasal septal deviation using tortuosity ratio from cone-beam computer tomography images. Computer Methods and Programs in Biomedicine 2020; 188: 105260.

[5] Gökçay B, Arda B. Tıp tarihi açısından uyku ve uyku araştırmaları. Mersin Üniversitesi Tıp Fakültesi Lokman Hekim Tıp Tarihi ve Folklorik Tıp Dergisi 2013; 3(1): 70-78.

[6] Hopkins C, Browne JP, Slack R, Lund V, Brown P. The Lund-Mackay staging system for chronic rhinosinusitis: how is it used and what does it predict? Otolaryngology-Head and Neck Surgery 2007; 137(4): 555-561.

[7] Wise SK, Lin SY, Toskala E, Orlandi RR, Akdis CA, Alt JA, ..., Zhang, L. International consensus statement on allergy and rhinology: allergic rhinitis. International Forum of Allergy & Rhinology 2018; 8(2): 108-352.

[8] Stewart MG, Smith TL, Weaver EM, Witsell DL, Yueh B, Hannley MT, Johnson JT. Outcomes after nasal septoplasty: results from the Nasal Obstruction Septoplasty Effectiveness (NOSE) study. Otolaryngology–Head and Neck Surgery 2004; 130(3), 283-290.

[9] Fokkens WJ, Lund VJ, Hopkins C, Hellings PW, Kern R, Reitsma S, ..., Zwetsloot CP. European position paper on rhinosinusitis and nasal polyps 2020. Rhinology, 2020: 58(Suppl S29): 1-464.

[10] Donovan LM, Boeder S, Malhotra A, Patel SR. New developments in the use of positive airway pressure for obstructive sleep apnea. Journal of Thoracic Disease 2015; 7(8): 1323.

[11] Epstein LJ, Kristo D, Strollo PJ, Friedman N, Malhotra A, Patil SP, ..., Weinstein MD. Clinical guideline for the evaluation, management and long-term care of obstructive sleep apnea in adults. Journal of Clinical Sleep Medicine 2009; 5(3): 263-276.

[12] Kryger MH, Roth T, Dement WC. Principles and practice of sleep medicine E-book: Expert consult-online and print. Elsevier Health Sciences 2010.

[13] Freedman N. Treatment of obstructive sleep apnea syndrome. Clinics in Chest Medicine 2010; 31(2): 187-201.

[14] Pazarli AC, Köseoğlu HI. Devices for CPAP in OSA. In Noninvasive Mechanical Ventilation: Theory, Equipment, and Clinical Applications 2023: 273-281. Cham: Springer International Publishing.

[15] Berry RB, Budhiraja R, Gottlieb DJ, Gozal D, Iber C, Kapur VK, ..., Tangredi MM. Rules for scoring respiratory events in sleep: Update of the 2007 AASM manual for the scoring of sleep and associated events. Journal of Clinical Sleep Medicine 2012; 8(5): 597-619.

[16] Sullivan C, Berthon-Jones M, Issa F, Eves L. Reversal of obstructive sleep apnoea by continuous positive airway pressure applied through the nares. The Lancet 1981; 317(8225): 862-865.

[17] Morgenthaler TI, Aurora RN, Brown T, Zak R, Alessi C, Boehlecke B, ..., Swick TJ. Practice parameters for the use of autotitrating continuous positive airway pressure devices for titrating pressures and treating adult patients with obstructive sleep apnea syndrome: an update for 2007. Sleep 2008; 31(1): 141-147.

[18] Rosen CL, Auckley D, Benca R, Foldvary-Schaefer N, Iber C, Kapur V, ..., Redline S. A multisite randomized trial of portable sleep studies and positive airway pressure autotitration versus laboratory-based polysomnography for the diagnosis and treatment of obstructive sleep apnea: the HomePAP study. Sleep 2012; 35(6): 757-767.

[19] Abbasnejad B, Thorby W, Razmjou A, Jin D, Asadnia M, Warkiani ME. MEMS piezoresistive flow sensors for sleep apnea therapy. Sensors and Actuators A: Physical 2018; 279: 577-585.

[20] Vardareli S, Çetin N, Hızal E, Büyüklü F, Alkan N,Yazıcı AC, Çakmak A. Nazal pasaj hacimlerinde egzersize bağımlı değişimlerin akustik rinometri ile ölçülmesi. Kulak Burun Boğaz ve Baş Boyun Cerrahisi Dergisi 2008; 16(1): 20-25.

[21] Sümbül H, Yüzer AH. Detection of respiratory signals according to different positions using acceleration sensor. In 2015 23nd Signal Processing and Communications Applications Conference (SIU), pp. 375-378, 2015, IEEE.

[22] Sheth R, Sheth S, Audette M. Developing custom-fit CPAP mask prototype in patients with obstructive sleep apnea. Journal of Sleep Research 2025; e70146.

[23] Etindele Sosso FA, Matos E. Socioeconomic disparities in obstructive sleep apnea: a systematic review of empirical research. Sleep and Breathing 2021; 25(4): 1729-1739.

[24] Guglielmi O, Lanteri P, Garbarino S. Association between socioeconomic status, belonging to an ethnic minority and obstructive sleep apnea: a systematic review of the literature. Sleep Medicine 2019; 57: 100-106.

[25] Isler Y, Cagatay OD. Design of Arduino shield to record real-time electrocardiography signals. In 6th International Symposium on Innovative Technologies in Engineering Science (ISITES-2018), 413-418, Alanya / Antalya / Turkey, 9-11 November 2018.

[26] Koo KY, Hester D, Kim S. Time synchronization for wireless sensors

using low-cost gps module and arduino. Frontiers in Built Environment 2019; 4: 82.

[27] Eker K, Kıymık MK. Design of a functional medical device for home monitoring. In 2016 Medical Technologies National Congress (TIPTEKNO),pp. 1-4, 2016, IEEE.

[28] Selek MB, Duyar MC, Isler Y. Electronic stethoscope design. Journal of Intelligent Systems with Applications 2020; 3(1): 10-16.

[29] Isler Y, Uzun YO. Yeni bir odyometri cihazı tasarımı. In 7th National Conference on Electrical, Electronics and Computer Engineering (ELECO2012), 2012, November, Bursa/Turkey (Vol. 29).

[30] Isler Y, Uzun YO. Farklı kaynaklara entegre işitme testi cihazı tasarımı, Tıp Teknolojileri Ulusal Kongresi (TIPTEKNO2016), Antalya / Turkey, 38-41, 27-29 October 2016.

[31] Sahin S, Isler Y, Selek MB. An example experiment in control of liquid level and temperature using virtual instruments. Celal Bayar Üniversitesi Soma Meslek Yüksekokulu Teknik Bilimler Dergisi 2007; 8(1): 1-10.

[32] Sahin S, Isler Y, Guzelis C. Chapter 19: A Real Time Simulation Platform for Controller Design, Test and Redesign, book chapter in Real-time Simulation Technologies: Principles, Methodologies, and Applications, ISBN: 978-1439846650, edited by K. Popovici and P.J. Mosterman, CRC Press, 461-499, 2012.

[33] Uzun R, Yaman GK, Tekkanat A, İşler Y. Wristband design to support blind people, 2017 Medical Technologies National Congress (TIPTEKNO), Trabzon, Turkey, 2017, pp. 1-4.

[34] Selek MB, Uzal VA, Isler Y. Arduino based probe bag alert system design. Journal of Intelligent Systems with Applications, 3(1): 20-24, 2020.

[35] Selek MB, Uzal VA, Isler Y. Arduino based probe bag alert system design. In 3rd International Conference on Medical Devices (ICMD'2020), Abstract Book, 21, Adrasan - Antalya / Turkey, 28-29 September 2020.

[36] Ciklacandir S, Isler Y. Design of a low-cost Arduino-based respiratory and sleep apnea detection system. Book of Abstracts, ISBN: 978-608-4868-02-6, 16, 2nd International Conference of Applied Sciences, Engineering and Mathematics (IBU-ICASEM 2020), June 4-6, Skopje/North Macedonia, 2020.